

Entrapment of Metal Nanoparticles in Polymer Stomatocytes

Daniela A. Wilson,* Roeland J. M. Nolte, and Jan C. M. van Hest*

Radboud University Nijmegen, Institute for Molecules and Materials, Heyendaalseweg 135, 6525 AJ, Nijmegen, The Netherlands

S Supporting Information

ABSTRACT: Polymersomes assembled from amphiphilic block copolymers containing a glassy hydrophobic segment can be further re-engineered to perform a controlled shape transformation from a thermodynamically stable spherical morphology to a kinetically trapped stomatocyte structure. The stable bowl-shape stomatocyte morphology is ideal for the specific physical entrapment of nanoparticles for potential use in heterogeneous catalysis and drug delivery. Herein we report two approaches to obtain a selective and controlled entrapment of platinum nanoparticles (PtNP) of different sizes and shapes inside the stomatocyte structure. In the first approach, the stomach of the stomatocytes is used to template the growth of the PtNP by controlling and confining the nucleation points inside the cavity. In the second method, preformed nanoparticles are engulfed during the stomatocyte formation process. Synergistically, the reverse effect is observed, that is, differently shaped nanoparticles were shown to exhibit a templating effect on the stomach formation of the stomatocytes.

Natural and synthetic amphiphiles,¹ amphiphilic block-copolymers,² and other compounds like amphiphilic Janus dendrimers³ are known to spontaneously self-assemble into nanosized architectures, called liposomes, vesicles, polymersomes, and dendrimersomes, respectively, which mimic the properties of biological membranes and cell organelles. Their spherical morphology can be reengineered via shape transformations triggered by either a change in the properties of the membrane (different spontaneous curvature) or through variation of external stimuli such as temperature or osmotic pressure. Such transformations⁴ have been demonstrated for the flexible and fluidic membranes of giant liposomes, although their presence was only transitory and difficult to preserve.

We recently reported that polymersomes containing a polystyrene segment can be forced to undergo shape transformation in a controlled manner from a spherical morphology to a bowl-shaped structure, called stomatocyte, and vice versa.⁵ This was achieved by applying an osmotic effect in the presence of a plasticizing organic solvent in water. Such a solvent increases the flexibility of the polymersome membrane, allowing it to distort when a change in the osmotic pressure is applied. Dialysis of such flexible polymersomes containing a plasticizing solvent results in a rapid extrusion of the solvent and the creation of a difference in osmotic pressure over the membrane. As a result, the inner volume of the polymersomes decreases, forcing the membrane to fold inward. After complete

removal of the solvent, the polystyrene segments in the membrane recover their rigidity and the stomatocyte becomes “locked in place”. Furthermore, these bowl shape structures were shown to self-propel in aqueous media, when catalytically active nanoparticles, trapped inside the stomach, decomposed hydrogen peroxide to produce a fast discharge of propelling oxygen gas.⁶

We envisioned that the extra inner compartment generated by the stomatocyte morphology coupled with the high stability of these glassy bowl-shaped stomatocyte architectures might be ideal for the entrapment of nanosized catalysts, nanoparticles, or other guest molecules. However, for selective entrapment and to prevent escape, control over the stomatocyte opening down to almost a closed structure would be needed, increasing significantly the utility of the stomatocyte inner compartment for encapsulation purposes. Although the embedding of metal nanoparticles within the hydrophobic or the hydrophilic pockets of liposomes or polymersomes was previously successful^{7,8} it also resulted in a destabilization of the membrane by either curving the membrane, or inducing budding, fusion or fission of vesicles.^{7c} However, the glassy membrane of the bowl shape stomatocytes was expected to prevent such effects. Poly(ethylene glycol)₄₄-*b*-polystyrene_{172–300} amphiphilic polymers having different lengths were synthesized and self-assembled using previously described procedures.^{5a,8a} Different tetrahydrofuran (THF)/dioxane solvent ratios were used for the self-assembly of the polymers in water to determine the ratio required to completely close the stomatocyte structure.⁶ In a typical procedure, the poly-(ethylene glycol)₄₄-*b*-polystyrene₁₇₇ amphiphilic block-copolymer (1 wt %) was dissolved in 2 mL of a mixture of THF/dioxane of different volume ratios, with THF varying from 55%, 70%, 80%, and further to 90% by volume. A fixed 50% volume of water was added slowly via a syringe pump using an addition rate of 1 mL/h. Polymersomes were immediately transferred into a dialysis bag and dialyzed against pure water. Higher content of THF preserved the flexibility of the membrane for a longer period of time during the shape transformation and resulted in a controlled decrease of the size of the opening from 100 nm for 55% THF down to less than 5 nm for 80% THF. A larger THF content (90 vol %) resulted in a completely closed stomatocyte structure with entirely fused membranes.⁶

Two approaches were envisaged for the selective and controlled entrapment of nanoparticles inside artificial stomatocytes (Figure 1). Nanoparticles can either be generated in the presence of preformed glassy stomatocytes, or preformed nanoparticles can be engulfed during the stomatocyte

Received: April 6, 2012

Published: June 7, 2012

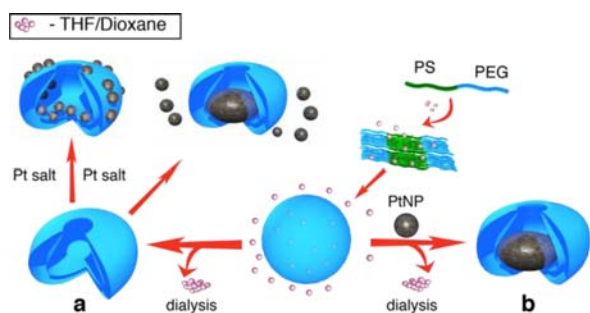


Figure 1. Strategies for the selective and controlled entrapment of platinum nanoparticles inside stomatocytes. (a) Nanoparticle-filled stomatocytes are formed via particle nucleation occurring inside the preformed stomatocyte cavity. (b) Nanoparticles are entrapped during the shape transformation of the polymersome.

formation process. Additionally, the confined space provided by the stomatocyte morphology might have a positive effect on the nucleation process by templating the growth of the nanoparticles. Vice versa, nanoparticles of different size and shape might also have a templating effect on the formation of the stomatocyte “stomach”. Herein we demonstrate this concept by selectively entrapping platinum nanoparticles of different sizes and shapes inside stomatocytes with a controlled opening, as well as the interaction of these particles with the stomatocyte membrane leading to a dual templating effect, both involving the stomatocyte nanocavity and the platinum nanoparticles.

The stomatocyte structures containing a narrow opening (less than 5 nm) were targeted as they allow for small substrate molecules to freely diffuse in and out of the stomatocyte nanocavity while keeping larger nanoparticles or guest molecules inside the stomatocyte stomach. For the first strategy of nanoparticle entrapment (pathway a in figure 1), we applied preformed stomatocytes, in which presence nanoparticles were grown. To obtain the required small opening, we used the 80% or 70% THF protocol (Figure 2 and Figures SF1–2).

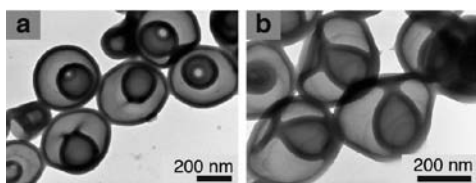


Figure 2. Stomatocytes obtained from the shape transformation of polymersomes assembled from poly(ethylene glycol)₄₄-b-polystyrene₁₇₇. TEM images showing the reduction of the size of the opening by increasing the volume percentage of THF compared to dioxane used for polymer dissolution and a fixed 50% water content for self-assembly (a) 70% THF, opening 20 nm; (b) 80% THF, opening less than 5 nm.

We also hypothesized that the stomach might have a templating effect on the formation of the nanoparticles by controlling and confining the nucleation. A large number of procedures for the synthesis of platinum nanoparticles with a strict control over size and shape have been reported in the literature.⁹ Among the methods available for nanoparticle formation, we focused on gentle methods that would be compatible with the polymeric building blocks of the stomatocytes and would provide high concentrations of water dispersible nanoparticles at room temperature. Chemical reduction of platinum salts in the presence of a water-soluble

capping agent necessary for colloidal stability can provide such large concentrations of nanoparticles of uniform size. The control of the size and shape of these structures is strongly dependent on the nature and the concentration of the platinum salt, the nature and concentration of the capping agents (surfactant or polymer), as well as the time allowed for nucleation and growth. We selected platinum nanoparticles (PtNP) because they have a rich morphology and are frequently used as catalysts in organic reactions.^{9,10} However, this strategy can be used for other metal nanoparticles as well. Platinum is a low-allergy metal with effective antioxidative properties that can efficiently quench reactive oxidative species.¹⁰ Sharp corners and edges, as well as high surface area provided by super branched morphologies, maximize the performance of the nanoparticles especially for catalytic applications.^{9a,10,11} Additionally, unconventional shapes such as cubes, hexagons, rods or dendrites are highly desirable to demonstrate the anticipated dual templating effect of the stomatocyte architecture on the final outcome of the nanoparticles, as well as the effect of the nanoparticles on the final result of the shape transformation.

Highly branched nanoparticles were recently prepared using the sonication technique,^{12a} while cubic structures were obtained by hydrogen reduction of the platinum salt under specific conditions of formation.^{12b} We modified these procedures by using different capping block-copolymer and polymer agents, that is, Pluronic F-127 (PEO₁₀₀PPO₆₅PEO₁₀₀), PVP (polyvinyl pyrrolidone), PEG_{3K}-(NH₂)₂, and PAA (sodium polyacrylate). These modified methods allowed us to generate nanoparticles of different sizes and shapes based on the original reports as well as nanoparticles with different charge and functionality on their surface. TEM and UV analysis confirmed the formation of the nanoparticles and complete reduction of the platinum salt (Figure SF3 and SF17).

The final size and shape of the nanoparticles was strongly dependent on the ratio of platinum salt to capping agent, the sonication time, the hydrogen flushing time, the concentration of the platinum salt and the nature of the capping agent (Supporting Information). To test the first strategy of entrapment, we employed the optimized procedures for the synthesis of the platinum nanoparticles, using both the sonication and hydrogen reduction methods in the presence of the stomatocytes. However, it was still expected that the presence of the stomatocytes in the reaction mixture along with the order of addition of the reagents would have an influence on the final shape and size of the nanoparticles. In the sonication method, we used both Pluronic F-127 and PVP as capping agents, ascorbic acid as reducing agent, and stomatocytes with different openings. Three different sequences of addition were tested, in which the stomatocytes were either mixed with the reducing agent or with the platinum salt or added at the end when nucleation had commenced (Figures SF4–7). In all three cases, a strong affinity of the nanoparticles with the stomatocyte membrane was observed, nucleation proceeding not only inside the stomach, but also on the membrane surface. However, several differences were noted. When the stomatocyte solution was mixed with the reducing agent and added at once to the platinum solution containing Pluronic F127, “mushroom”-like structures growing on the stomatocyte surface were observed (Figure SF4). In this case, nucleation occurred on the surface with formation of large dendritic hemispheres, as shown by both TEM and SEM observations (Figure SF4). Addition of the stomatocyte

solution after the platinum salt had been mixed with the reducing agent generated dendritic nanoparticles with the same size and shape as observed in the synthesis of nanoparticles without stomatocytes. However TEM and SEM analysis showed the same strong affinity of the nanoparticles with the membrane as well as a uniform distribution of the nanoparticles on the stomatocyte surface (Figure 3, Figures S5–7, SF12).

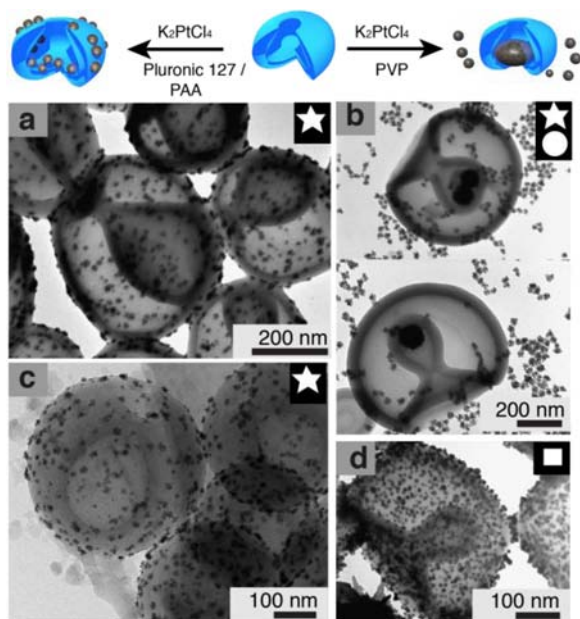


Figure 3. Templating effect of the stomatocyte stomach. In situ formation of platinum nanoparticles in stomatocytes via sonication or the hydrogen reduction method. (a and c) TEM and cryo-TEM images of stomatocytes covered uniformly with dendritic PtNP. The following sequence of addition was employed: stomatocytes were added after the solution of platinum salt and Pluronic F-127 had been mixed with the reducing agent (addition after the nucleation started). (b) TEM image of in situ formed PtNP containing PVP as capping agent using the sonication method. The same sequence of addition as in (a) was employed. Larger nanoparticles are formed inside the stomach compared to the nanoparticles formed in solution. (d) TEM image of in situ formed PtNP containing PAA as capping agent using the hydrogen reduction method. Insets show schematically the final shape of the nanoparticles.

Since the size and the shape of the nanoparticles obtained in this case were the same as obtained without stomatocytes, we used the same sequence of addition for all the other in situ procedures. The hydrogen reduction method for the synthesis of cubic nanoparticles using PAA as capping agent was also performed in the presence of stomatocytes. The morphology of the cubic nanoparticles was not altered by their presence and the same strong interaction with the membrane and nucleation on the stomatocyte surface was observed. Moreover, while the shape was not affected, smaller size nanoparticles were found to nucleate onto the membrane whereas larger nanoparticles were observed in solution (Figure SF11).

Changing of the capping agent to PVP in the sonication experiment prevented interaction of the formed nanoparticles with the stomatocyte membrane. Remarkably, only one nanoparticle and rarely two were formed inside the stomach and their size was considerably larger than the size of the particles observed outside the cavity (Figure 4c and Figures SF8–10). Therefore, the “stomach” of the stomatocyte has a

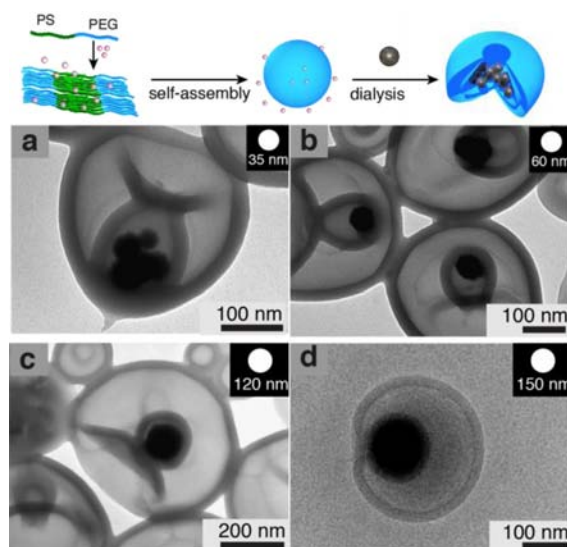


Figure 4. Encapsulation of platinum nanoparticles inside stomatocytes. TEM images of stomatocytes entrapping preformed platinum nanoparticles of different size (a) 35 nm PVP-capped PtNP, (b) 60 nm PVP-capped PtNP, (c) 120 nm PVP-capped PtNP, (d) cryo-TEM image of stomatocyte entrapping 150 nm PVP-capped PtNP. Stomatocyte formation followed the 80% THF volume protocol.

templating effect on the growth of the PtNP. This is indeed a truly physical templating effect of the nanocavity rather than “growth directing” effect as observed in the previous case of nanodendrites templated by liposomes.^{7d} It is most probable that the nucleation proceeds at different rates inside the stomatocytes when compared to the surrounding solution. This is due to the lower concentrations of the platinum salt and the capping agent inside the cavity, which generates fewer nucleation points and therefore facilitates the growth of larger particles. On the other hand, the presence of a larger number of nuclei in the outside environment coupled with the greater availability of the capping agent results in smaller dendritic structures in the exterior media. It is well-known that the size of nanoparticles is strongly dependent on the surrounding capping agent concentration. When PVP is abundant in the solution, it absorbs quickly onto the Pt nuclei resulting in smaller size nanoparticles. Inside the stomatocyte nanocavity, the presence of the PVP is diffusion-limited, and therefore, the particles are expected to grow larger. Furthermore, UV analysis of all the in situ prepared nanoparticles showed no presence of platinum(II) in solution and complete reduction of platinum salt (Suppl. Figure S3).

In the second strategy (route b in Figure 1) to encapsulate nanoparticles, we made use of the flexible membrane structure of the polymersomes in the “unlocked” state and the possibility to perform the shape transformation in the presence of a high concentration of preformed platinum nanoparticles allowing these particles to be “swallowed” during the transformation process. In this case, the nanoparticles may also interact with the stomatocyte membrane depending on the nature and the charge of the capping agents. Since PVP PtNPs were previously shown not to interact with the stomatocyte membrane, we used PVP nanoparticles of different sizes to test this second approach of encapsulation. During the transition from the flexible to the glassy state, nanoparticles differing in size from 30 to 150 nm were engulfed inside the stomatocyte pockets, as was clear from TEM analysis (Figure 4 and Figures SF13–16).

We anticipated that the size and the shape of the nanoparticles could affect the stomatocyte formation process. Indeed a surprising effect was observed when relatively large PtNPs, that is, of sizes of ca. 100 nm were used for encapsulation. In this case, only one particle was engulfed inside the stomach during the inward folding of the polymersome membrane and the mouth of the stomatocyte structure was nearly completely closed. It can therefore be concluded that the stomatocyte stomach was templated by the size and the shape of the nanoparticles used for the encapsulation (Figure 4c,d; Figures SF13–14). This remarkable entrapment behavior mimics phagocytosis, a form of endocytosis occurring in cells by which large solid particles are engulfed by the cell membrane and internalized.

In conclusion, we have demonstrated that platinum nanoparticles can be selectively entrapped inside the stomach of artificial stomatocytes and that control over both the entrapment and the opening of stomatocytes can be obtained. We have achieved this by following two methods, either by directly using the confined space provided by the stomatocytes for nanoparticle formation or by performing the shape transformation in the presence of preformed nanoparticles. A dual templating effect of both the stomatocyte nanocavity and the nanoparticles was observed. The stomatocyte was found to control the nucleation process inside the nanocavity, which is of use not only for nanoparticle formation, but also for other applications requiring control over nucleation such as protein crystallization. When sufficiently large, the nanoparticles were shown to template the size and shape of the stomatocyte's stomach. Additionally, nanoparticles with different capping agents behaved differently in the presence of the stomatocytes, either interacting with the membrane by nucleating on the surface or completely repelling the membrane. The controlled entrapment of nanoparticles inside stomatocytes adds a new dimension of functionality to these structures by taking advantage not only of the confinement offered by the stomach, but also of the additional properties provided by the entrapped structures. This encapsulation methodology can be applied not only to Pt nanoparticles, but also to other types of metal catalysts and guest molecules. Besides their obvious catalytic application as nanoreactors in heterogeneous catalysis, these "loaded stomatocytes" can be seen as an example of the "ship-in-a-bottle" concept, which opens interesting possibilities for designing new drug delivery systems.

■ ASSOCIATED CONTENT

Supporting Information

Additional information regarding polymer synthesis and self-assembly coupled with detailed TEM, cryo-TEM and SEM images of stomatocytes entrapping platinum nanoparticles. This material is available free of charge via the Internet at <http://pubs.acs.org>.

■ AUTHOR INFORMATION

Corresponding Author

d.wilson@science.ru.nl; j.vanhest@science.ru.nl

Notes

The authors declare no competing financial interest.

■ ACKNOWLEDGMENTS

This work was supported by the Dutch Science Foundation under the VICI-project Kinetically controlled peptide-polymer

artificial organelles. D.A.W. and R.J.M.N. acknowledge financial support from the Royal Netherlands Academy of Science. The authors would like to thank to Dr. Matthijn Vos and Dr. Jason Pierson for technical support with cryo-TEM.

■ REFERENCES

- (1) Bangham, A. D.; Standish, M. M.; Watkins, J. C. *J. Mol. Biol.* **1965**, *13*, 238.
- (2) (a) Discher, B. M.; Won, Y.-Y.; Ege, D. S.; Lee, J. C.-M.; Bates, F. S.; Discher, D. E.; Hammer, D. A. *Science* **1999**, *284*, 1143. (b) Discher, D. E.; Eisenberg, A. *Science* **2002**, *297*, 967. (c) van Dongen, S. F. M.; De Hoog, H. P. M.; Peters, R. J. R. W.; Nallani, M.; Nolte, R. J. M.; Van Hest, J. C. M. *Chem. Rev.* **2009**, *109*, 6212. (d) Rosen, B. M.; Wilson, C. J.; Wilson, D. A.; Imam, M. R.; Peterca, M.; Percec, V. *Chem. Rev.* **2009**, *109*, 6275.
- (3) Percec, V.; Wilson, D. A.; Leowanawat, P.; Wilson, C. J.; Hughes, A. D.; Kaucher, M. S.; Hammer, D. A.; Levine, D. H.; Kim, A. J.; Bates, F. S.; Davis, K. P.; Lodge, T. P.; Klein, M. L.; DeVane, R. H.; Aqad, E.; Rosen, B. M.; Argintaru, A. O.; Sienkowska, M. J.; Rissanen, K.; Nummelin, S.; Ropponen, J. *Science* **2010**, *328*, 1009.
- (4) (a) Hotani, H. *J. Mol. Biol.* **1984**, *178*, 113. (b) Käs, J.; Sackmann, E. *Biophys. J.* **1991**, *60*, 825. (c) Yanagisawa, M.; Imai, M.; Taniguchi, T. *Phys. Rev. Lett.* **2008**, *100*, 148102. (d) Seifert, U. *Adv. Phys.* **1997**, *46*, 13. (e) Lipowsky, R. *Nature* **1991**, *349*, 475.
- (5) (a) Kim, K. T.; Zhu, J.; Meeuwissen, S. A.; Cornelissen, J. J. L. M.; Pochan, D. J.; Nolte, R. J. M.; van Hest, J. C. M. *J. Am. Chem. Soc.* **2010**, *132*, 12522. (b) Meeuwissen, S. A.; Kim, K. T.; Chen, Y.; Pochan, D. J.; van Hest, J. C. M. *Angew. Chem., Int. Ed.* **2011**, *50*, 1.
- (6) For use of platinum encapsulated stomatocytes as motor systems, see (a) Wilson, D. A.; Nolte, R. J. M.; van Hest, J. C. M. *Nat. Chem.* **2012**, *4*, 268. (b) Howse, J. *Nat. Chem.* **2012**, *4*, 247.
- (7) (a) Chen, R.; Pearce, D. J. G.; Fortuna, S.; Cheung, D. L.; Bon, S. A. F. *J. Am. Chem. Soc.* **2011**, *133*, 2151. (b) Hickey, R. J.; Haynes, A. S.; Kikkawa, J. M.; Park, S.-J. *J. Am. Chem. Soc.* **2011**, *133*, 1517. (c) Schultz, M.; Olubummo, A.; Binder, W. H. *Soft Matter* **2012**, *8*, 4849. (d) Song, Y.; Yang, Y.; Medforth, C. J.; Pereira, E.; Singh, A. K.; Xu, H.; Jiang, Y.; Brinker, C. J.; van Swol, F.; Shelnutz, J. A. *J. Am. Chem. Soc.* **2004**, *126*, 635. (e) Kumar, R. K.; Yu, X.; Patil, A. J.; Li, M.; Mann, S. *Angew. Chem., Int. Ed.* **2011**, *50*, 9343.
- (8) (a) Yu, Y.; Eisenberg, A. *J. Am. Chem. Soc.* **1997**, *119*, 8383. (b) Mai, Y.; Eisenberg, A. *J. Am. Chem. Soc.* **2010**, *132*, 10078. (c) Mai, Y.; Eisenberg, A. *Macromolecules* **2011**, *44*, 3179. (d) Guo, Y.; Saei, S.; Izumu, C. M. S. *ACS Nano* **2011**, *5*, 3309.
- (9) (a) Kotov, N. *Science* **2010**, *330*, 188. (b) Burda, C.; Chen, X.; Narayanan, R.; El-Sayed, M. A. *Chem. Rev.* **2005**, *105*, 1025. (c) Witham, C. A.; Huang, W. Y.; Tsung, C. K.; Kuhn, J. N.; Somorjai, G. A.; Toste, F. D. *Nat. Chem.* **2010**, *2*, 36. (d) Yamada, Y.; Tsung, C.-K.; Huang, W.; Huo, Z.; Habas, S. E.; Soejima, T.; Aliaga, C. E.; Somorjai, G. A.; Yang, P. *Nat. Chem.* **2011**, *3*, 372.
- (10) (a) Onizawa, S.; Aoshiba, K.; Kajita, M.; Miyamoto, Y. *Pulm. Pharmacol. Ther.* **2009**, *22*, 340. (b) Liu, X.; Wie, W.; Wang, C.; Yue, H.; Ma, D.; Zhu, C.; Ma, G.; Du, Y. *J. Mater. Chem.* **2011**, *21*, 7105. (c) Shimakoshi, H.; Hisaeda, Y.; Shirahata, S. *Langmuir* **2008**, *24*, 7354.
- (11) (a) Xia, Y.; Lim, B. *Nature* **2010**, *467*, 923. (b) Hickey, R. J.; Haynes, A. S.; Kikkawa, J. M.; Park, S.-J. *J. Am. Chem. Soc.* **2011**, *133*, 1517.
- (12) (a) Wang, L.; Yamauchi, Y. *J. Am. Chem. Soc.* **2009**, *131*, 9152. (b) Ahmadi, T. S.; Wang, Z. L.; Green, T. C.; Henglein, A.; El-Sayed, M. A. *Science* **1996**, *272*, 1924.